A new calibration setup for lock-in amplifiers in the low frequency range and its validation in a bilateral comparison

A new calibration setup for lock-in amplifiers in the low frequency range and its validation in a bilateral comparison

Alessandro Cultrera[1], David Corminboeuf[2], Vincenzo D'Elia[1], Ngoc Thanh Mai Tran[1,3], Luca Callegaro[1], and Massimo Ortolano[2]

[1]INRIM — Istituto Nazionale di Ricerca Metrologica
Strada delle Cacce, 91, 10135 Torino, Italy

[2] METAS — Swiss Federal Institute of Metrology
3003 Bern, Switzerland

[3] Politecnico di Torino
Corso Duca degli Abruzzi 24, 10129 Torino, Italy

E-mail: a.cultrera@inrim.it

Abstract. This paper addresses the calibration of lock-in amplifiers in the low frequency range. A simple but effective calibration setup implemented at INRIM is described. This includes a stable low-voltage source, composed of a digital sine wave generator and a cascade of two voltage dividers, one inductive and one resistive. The magnitude error is the lock-in magnitude error, which can be determined with an uncertainty of the order of 10^{-4} or better, that is, two orders of magnitude lower than the typical lock-in accuracy specification. The system can operate with an input voltage from 0.1 µV to 10 µV and a frequency from a few hertz to about 1 kHz. The performances of the calibration setup were evaluated at 1 µV and 10 µV at 20 Hz and 103 Hz and compared with those of another existing setup, implemented at METAS, through a direct comparison in the framework of a EURAMET Research Project.

Submitted to: *Metrologia*

1. Introduction

Lock-in amplifiers [1–4] are instruments that can recover, by homodyne detection, the component at frequency f of a small input signal, possibly corrupted by interference and noise. As vector meters, lock-in amplifiers measure the magnitude and phase of this component. The information about f is provided by the operator with a large signal at the reference input of the instrument.

Lock-in amplifiers are widely employed in experiments as signal recovery instruments, to measure very small signals with amplitudes down to the nanovolt range. They are not designed to be precision instruments: in fact, the typical specifications for the gain accuracy are of the order of percent. A calibration of the lock-in amplifier gain can reduce the measurement uncertainty of many experiments. However, to the authors' knowledge, the literature about the calibration of lock-in amplifiers is scant [5–8].

We describe here a simple setup for the calibration of the gain of a lock-in amplifier, for voltage ranges from 1 µV to 100 µV and frequency from a few hertz to about 1 kHz. These amplitude and frequency ranges are typical in the application of lock-in amplifiers to physics experiments [9–15], in the case of both commercial instruments and purpose-built devices. The evaluation of the system was performed at 1 µV and 10 µV, at 20 Hz and 103 Hz.

The setup herewith described, implemented at the Istituto Nazionale di Ricerca Metrologica (INRIM), was involved in a bilateral international comparison with the Swiss Federal Institute of Metrology (METAS). Two digital lock-in amplifiers were calibrated with both the proposed system and the one developed at METAS [7], with a relative accuracy in the 10^{-4} range. The outcome of the comparison is reported and discussed.

2. Setup

The coaxial schematic diagram of the calibration setup is shown in figure 1, and a photograph in figure 2. Table 1 lists the equipment employed.

A multichannel digital-to-analog converter board G generates large periodic voltage signals at the test frequency f. Channel 1 drives the input of the amplifier A with a low-distortion sine wave. In the following, sinusoidal voltage signals are represented by complex phasors, normalized so that phasor magnitudes correspond to rms values. The rms value $|V_\mathrm{S}|$ of the amplifier output voltage V_S is measured by the calibrated voltmeter V. The amplifier drives also the input of an inductive voltage divider IVD set for a ratio k_IVD. The IVD output is further scaled by a factor k_RVD by the resistive voltage divider RVD, composed of the two calibrated resistors R_1 and R_2. The choice of using cascaded IVD and RVD is due to the fact that with two cascaded RVDs there is a larger loading error. On the other hand, an accurate IVD with such a large ratio should be designed on purpose, which is not in the rationale behind this setup. The output voltage V_CAL of RVD, with rms value $|V_\mathrm{CAL}|$, is the calibration signal for the lock-in amplifier DUT. Figure 1 shows the connection of R_2, defined as a four terminal-pair resistor, to a DUT with a differential input. If a single-ended input is available, a four terminal coaxial connection [4] can be employed. Channel 2 of G generates the signal driving the reference input REF of DUT. In the experiments performed, this signal is a symmetric square wave of amplitude 4 V peak to peak. Channel 3 generates a TTL-compatible signal applied to the trigger input EXT TRIG of V.

A personal computer (not shown in figure 1) controls G via a PCI bus, and V, IVD and DUT via a GPIB interface.

3. Measurement model

The objective of this section is to provide a suitable definition of the magnitude error of the lock-in amplifier and a corresponding measurement model. Other definitions, more general and including the phase error or tailored to specific applications, are possible as well.

The lock-in amplifier DUT determines the input signal with respect to an internal reference signal, which can be shifted with respect to the external reference signal applied to the input REF by a phase angle $-\varphi$, settable by the operator. In the setup of figure 1, the external reference phase coincides with that of V_S. Therefore, with respect to the internal reference and compensating for a possible phase error, we can define the calibration signal as

$$V_\mathrm{CAL} = |k_\mathrm{RVD}||k_\mathrm{IVD}||V_\mathrm{S}|\mathrm{e}^{\mathrm{j}\varphi}, \tag{1}$$

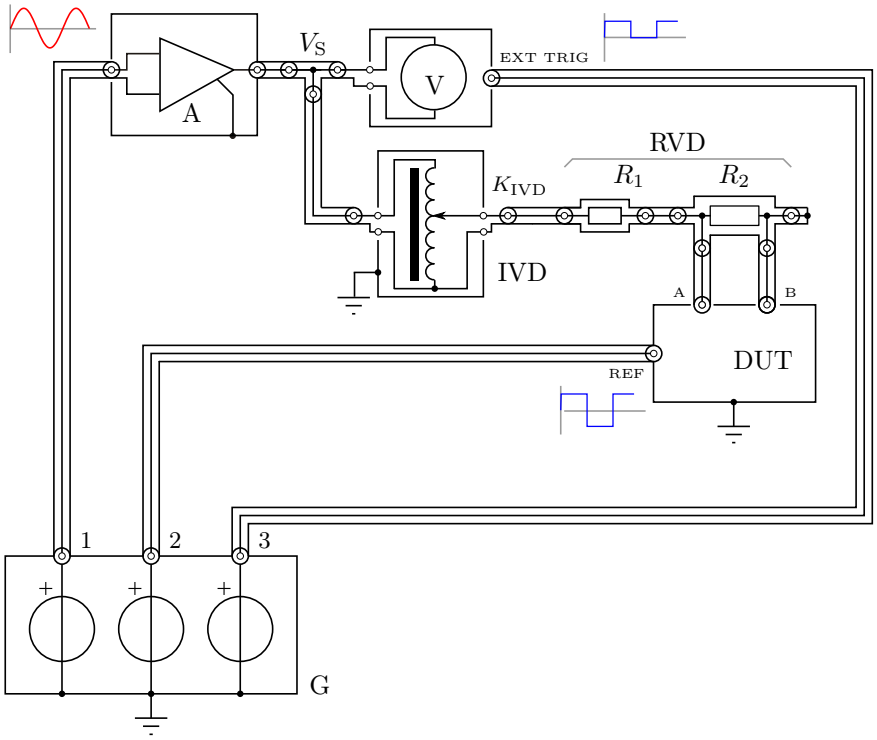

Figure 1. Schematic diagram of the calibration setup. Legend of the labels employed is given in Sec. 2 and Tab. 1.

Table 1. Equipment employed in the setup of figure 1.

Symbol	Instrument	Model
G	Generator	National Instruments PCI-6733, 10 V range, 16 bit resolution
A	Amplifier	Unity-gain custom buffer amplifier with differential input
V	Voltmeter	Keysight 3458A multimeter, AC voltage function, SYNC mode, TRIG EXT mode, ACBAND (1–200) Hz
IVD	Inductive voltage divider	Electro Scientific Instruments PRT-73, 7-decade automatic precision ratio transformer, 2.5 V/Hz option
RVD	Resistive ratio divider	Composed of R_1 and R_2
R_1	100 kΩ resistor	New Resistance A02 series resistor defined as two-terminal pair standard with BPO MUSA connectors
R_2	1 Ω and 10 Ω resistors	Vishay H series resistors defined as four terminal-pair standards with BPO MUSA connectors

with

$$k_{\mathrm{RVD}} = \frac{1}{1+\dfrac{R_1}{R_2}\left(1+\dfrac{R_2}{R_{\mathrm{in}}}+\mathrm{j}\omega R_2 C_{\mathrm{in}}\right)} \tag{2}$$

$$\approx \frac{1}{1+R_1/R_2}\,\frac{1}{1+\mathrm{j}\omega R_2 C_{\mathrm{in}}}, \tag{3}$$

where R_{in} and C_{in} represent the parallel input resistance and capacitance of DUT, respectively, including the interconnecting cable capacitance, and $\omega = 2\pi f$. The last approximation (3) is valid when $R_{\mathrm{in}} \gg R_1 \gg R_2$.

The DUT input voltage V_{DUT}, which is the differential voltage between the inputs A and B, can be affected by an offset voltage V_{OS} due to the possible electromagnetic coupling from V_{S} to V_{CAL} and those internal to DUT. Thus, $V_{\mathrm{DUT}} = V_{\mathrm{CAL}} + V_{\mathrm{OS}}$. Under the assumption that V_{OS} is independent of k_{IVD}, the measurement can be then performed in two steps, one with k_{IVD} set to the value of interest, with corresponding reading $V_{\mathrm{DUT}}^{\mathrm{read}}$, and one with k_{IVD} set to 0, with corresponding reading $V_{\mathrm{OS}}^{\mathrm{read}}$. The calibration signal read by DUT can be then defined as

$$V_{\mathrm{CAL}}^{\mathrm{read}} = |V_{\mathrm{DUT}}^{\mathrm{read}} - V_{\mathrm{OS}}^{\mathrm{read}}|\mathrm{e}^{\mathrm{j}\varphi}. \tag{4}$$

With the above definitions, the relative magnitude error of DUT is

$$\delta_{\mathrm{R}} = \frac{V_{\mathrm{CAL}}^{\mathrm{read}} - V_{\mathrm{CAL}}}{V_{\mathrm{CAL}}} = \frac{|V_{\mathrm{DUT}}^{\mathrm{read}} - V_{\mathrm{OS}}^{\mathrm{read}}|}{|k_{\mathrm{IVD}}||k_{\mathrm{RVD}}||V_{\mathrm{S}}|} - 1. \tag{5}$$

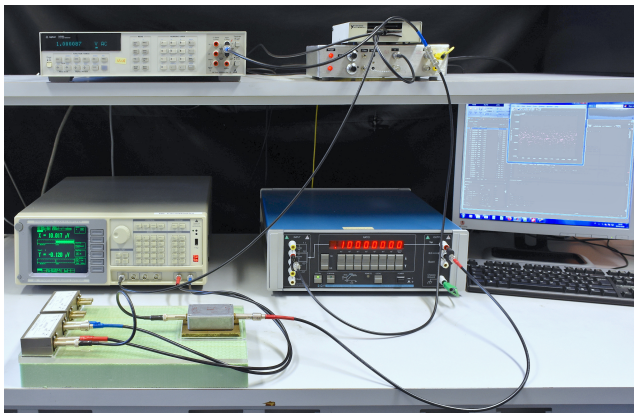

Figure 2. Photograph of the measurement setup of figure 1.

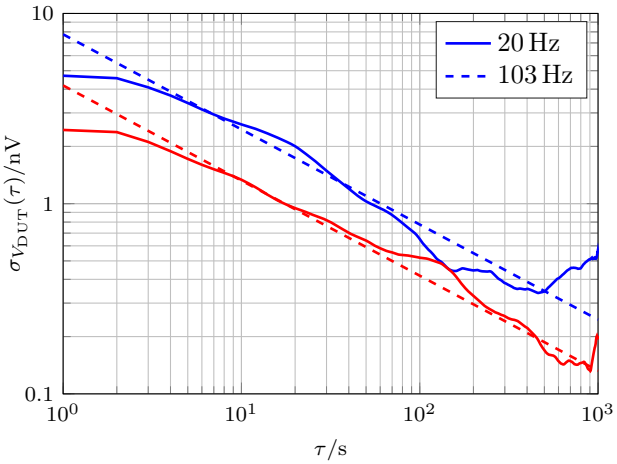

Figure 3. Allan deviation of the lock-in readings $V_{\mathrm{DUT}}^{\mathrm{read}}$ for $V_{\mathrm{CAL}} = 1\,\mu\mathrm{V}$ at 20 Hz and 103 Hz. Data fit to $\tau^{-1/2}$ in the range from 3 s to 200 s are also plotted as dashed lines.

The magnitude error can also be defined relatively to the full-scale range V_{FS} (a positive real quantity) of DUT,

$$\delta_{\mathrm{FS}} = \frac{|V_{\mathrm{DUT}}^{\mathrm{read}} - V_{\mathrm{OS}}^{\mathrm{read}}| - |k_{\mathrm{IVD}}||k_{\mathrm{RVD}}||V_{\mathrm{S}}|}{V_{\mathrm{FS}}} \mathrm{e}^{\mathrm{j}\varphi}, \qquad (6)$$

In the following, we restrict the analysis to φ set to either 0 or π, such that $\mathrm{e}^{\mathrm{j}\varphi} = \pm 1$.

4. Operation and performance

The setup was tested with a popular commercial lock-in amplifier as DUT, the Stanford Research Systems SR850. Table 2 reports the settings of DUT, which were also employed in the comparison described in the referenced section. The generator G was set to synthesize a sine wave with $|V_{\mathrm{S}}| = 1\,\mathrm{V}$ at the frequencies $f = 20\,\mathrm{Hz}$ or $f = 103\,\mathrm{Hz}$, with 1000 samples per period. The 103 Hz frequency was chosen to avoid interference from the 50 Hz power line. The reading mode XY has been employed.

We tested DUT at the ranges of 1 µV and 10 µV. For the 1 µV range, we chose $R_2 = 1\,\Omega$ such that $k_{\mathrm{RVD}} = 10^{-5}$. For the 10 µV range, we chose $R_2 = 10\,\Omega$ such that $k_{\mathrm{RVD}} = 10^{-4}$. In both cases, during the calibration, k_{IVD} was then varied from 0.01 to 0.1 in 0.01 steps, typically for both $\varphi = 0$ and $\varphi = \pi$.

Figure 3 reports the Allan deviation $\sigma_{V_{\mathrm{DUT}}^{\mathrm{read}}}(\tau)$ of $V_{\mathrm{DUT}}^{\mathrm{read}}$ for $|V_{\mathrm{CAL}}| = 1\,\mu\mathrm{V}$ at 20 Hz and 103 Hz. Both curves show approximately $\sigma_{V_{\mathrm{DUT}}^{\mathrm{read}}}(\tau) \propto \tau^{-1/2}$ from about 3 s to (200–300) s, typical of white noise. The deviation from the white-noise reference line below 3 s is due to the lock-in filter response and time constant [16]. The same behaviour was observed for $|V_{\mathrm{CAL}}| = 10\,\mu\mathrm{V}$.

4.1. Traceability and uncertainty

The traceability of V_{CAL} stems from the calibration of the individual components of (1). An example of uncertainty budget for this quantity is reported in table 3.

Table 2. DUT settings used for the bilateral comparison.

Parameter	Setting
Input configuration	A − B float
Reading mode	XY
Coupling	AC
Reference source	External at 20 Hz or 103 Hz
Sensitivity V_{FS}	1 µV or 10 µV
Time constant	300 ms
Low pass filter slope	24 dB/oct
Synchronous filter	Off
Reference phase shift	0°
Reserve mode	Low noise
Line notch filters	Off
Sampling rate	1 Hz
Sine output level	Minimum

Table 3. Uncertainty budget for $|V_{\mathrm{CAL}}| = 1\,\mu\mathrm{V}$, $V_{\mathrm{FS}} = 10\,\mu\mathrm{V}$, $f = 103\,\mathrm{Hz}$.

Quantity	x_i	$u(x_i)$	Type	$u_i(\lvert V_{\mathrm{CAL}}\rvert)$
$\lvert V_{\mathrm{S}}\rvert$	1.000 140 V	64 µV	B	64 pV
$\lvert k_{\mathrm{IVD}}\rvert$	0.010 000	5×10^{-7}	B	50 pV
$\lvert k_{\mathrm{RVD}}\rvert$	$9.999\,28 \times 10^{-5}$	1.3×10^{-9}	B	10 pV
$\lvert V_{\mathrm{CAL}}\rvert$	1 µV			82 pV [82×10^{-6}]

V was calibrated with traceability to the Italian national standard of ac voltage [17]. Three-month specifications from calibration were considered.

k_{IVD} : specifications and factory calibration show that the deviations of the real part $\mathrm{Re}\,k_{\mathrm{IVD}}$ of k_{IVD} from the nominal value are of a few parts in 10^7 or less. In the frequency range of interest

for this work, up to 1 kHz, the imaginary part is typically sufficiently small. In the instrument specifications, a phase error $\varphi_{\mathrm{IVD}} \approx \pm 20\,\mu\mathrm{rad}$ is given at 100 Hz. At 10 Hz, the phase error increases to 200 µrad. This phase error enters in quadrature in the magnitude,

$$|k_{\mathrm{IVD}}| = \frac{\mathrm{Re}\, k_{\mathrm{IVD}}}{\cos\varphi_{\mathrm{IVD}}} \approx \mathrm{Re}\, k_{\mathrm{IVD}} \left(1 + \frac{\varphi_{\mathrm{IVD}}^2}{2}\right) \qquad (7)$$

and its contribution is less than 2×10^{-8} in the worst case such that $|k_{\mathrm{IVD}}| \approx \mathrm{Re}\, k_{\mathrm{IVD}}$ within the specified accuracy of the real part. A conservative uncertainty $u(|k_{\mathrm{IVD}}|) = 5 \times 10^{-7}$ was considered, including the effect of the loading from RVD. Drifts in time or due to transportation of IVDs are known to be extremely small (see [18], part 2, section 1.2), as well as the temperature coefficient (10^{-8}/K or below for DT72, the manual version of the IVD here considered [19]) and can therefore be neglected.

k_{RVD} The resistors R_1 and R_2 are measured as two-terminal (R_1) or four-terminal (R_2) standards in dc, with a calibrated precision multimeter. The measurement is traceable to the Italian national standard of dc resistance [20]. The ac-dc differences and time constants of R_1 and R_2 are negligible in the frequency range here considered [21] for the calibration of the lock-in amplifiers. The magnitude of k_{RVD}, since $R_1 \gg R_2$, can be approximated to $k_{\mathrm{RVD}} \approx \frac{R_2}{R_1+R_2}[1 + \frac{1}{2}\omega^2(\tau_2 - \tau_1)^2)]$; given the resistors values and specifications [22], we take $-\tau_1 = R_1 C < 100\,\mathrm{ns}$ and $\tau_2 = L/R_2 < 10\,\mathrm{ns}$, that returns a ratio error magnitude of less than 10×10^{-6}.
For the typical DUT considered [23], $R_{\mathrm{in}} = 10\,\mathrm{M}\Omega$ and taking into account the interconnection capacitance, we can consider $C_{\mathrm{in}} < 100\,\mathrm{pF}$, such that $\omega R_2 C_{\mathrm{in}} < 6 \times 10^{-6}$. From (2), these yield an error on $|k_{\mathrm{RVD}}|$ less than 10^{-6}, negligible with respect to the calibration uncertainty of RVD.

5. INRIM-METAS comparison: the EURAMET 1466 project

The performance of the INRIM calibration setup proposed in the previous sections was compared with a setup [7] developed by METAS. The comparison was framed within a European Association of National Metrology Institutes (EURAMET) Cooperation in Research project, n. 1466 [24].

5.1. The METAS calibration setup

The METAS setup shown in figure 4 is based on cascaded inductive voltage dividers (IVDs). The three active transformers T1, T2 and T3, described in detail in [7], are two-stage, double-shielded transformers. A very low noise JFET operational amplifier mounted as buffer drives the magnetizing winding; this increases the input impedance of the two-stage transformer, thus avoiding an excessive load that would degrade the ratio of the previous stage. Each active transformer has a 10 : 1 ratio and can work at frequencies from 20 Hz to 10 kHz at a maximum rating of 0.08 V/Hz. The reference divider ($\mathrm{IVD_{REF}}$) is a two-stage, single-shielded divider with 8 decades for measurements at 103 Hz. At 20 Hz, a Siemens D521 IVD was used instead to reduce the harmonic distortion of the output signal.

The two DACs outputs of a PXI board, a National Instruments NI PXI 4461, were used as signal generators, the first one as the voltage source with a signal amplitude of 50 mV. The second output, perfectly synchronous with the first one, was used to generate the reference signal of the lock-in amplifier with a constant signal amplitude of 1 V. Another PXI board, the NI PXI 6220, was used as a clock generator for the voltmeter HP 3458A to ensure synchronization between the voltmeter and the source signal. The voltmeter was used in the digitizing mode to reach an uncertainty of 10 µV/V in the 100 mV range, better than that in the AC mode. The amplitude of the signal was calculated with a Fast Fourier Transform (FFT) algorithm. At 20 Hz, the sampling frequency of the voltmeter at the EXT TRIG input was 4000 Hz and at 103 Hz, this frequency was 4120 Hz but in both cases, the number of acquired samples was 800. This relatively small number of samples is due to the low reading rate of the voltmeter as the goal was to achieve one measurement per second.

5.2. The comparison

The comparison took place in February 2020 at METAS. The INRIM system was moved there. Two Stanford Research Systems SR850 units (LIA1 and LIA2 in the following) were calibrated by both the INRIM and METAS setups within a short time interval. Each measurement, performed at given range V_{FS} and frequency f, took about 40 min. The DUT's measurement settings used for this comparison are given in table 2 in section 4.

The outcome of the comparison, in terms of the magnitude errors δ_{R} and δ_{FS}, defined by (5) and (6), respectively, is reported for each DUT and both calibration setups in figures 5 and 6. The plots in figure 5 report δ_{R} and δ_{FS} at $f = 20\,\mathrm{Hz}$ while the plots in figure 6 correspond to $f = 103\,\mathrm{Hz}$. The results from the INRIM setup are reported in blue, those from the METAS setup in red.

For each V_{FS} and f a number of calibration points are presented. The values on the V_{CAL} axis are

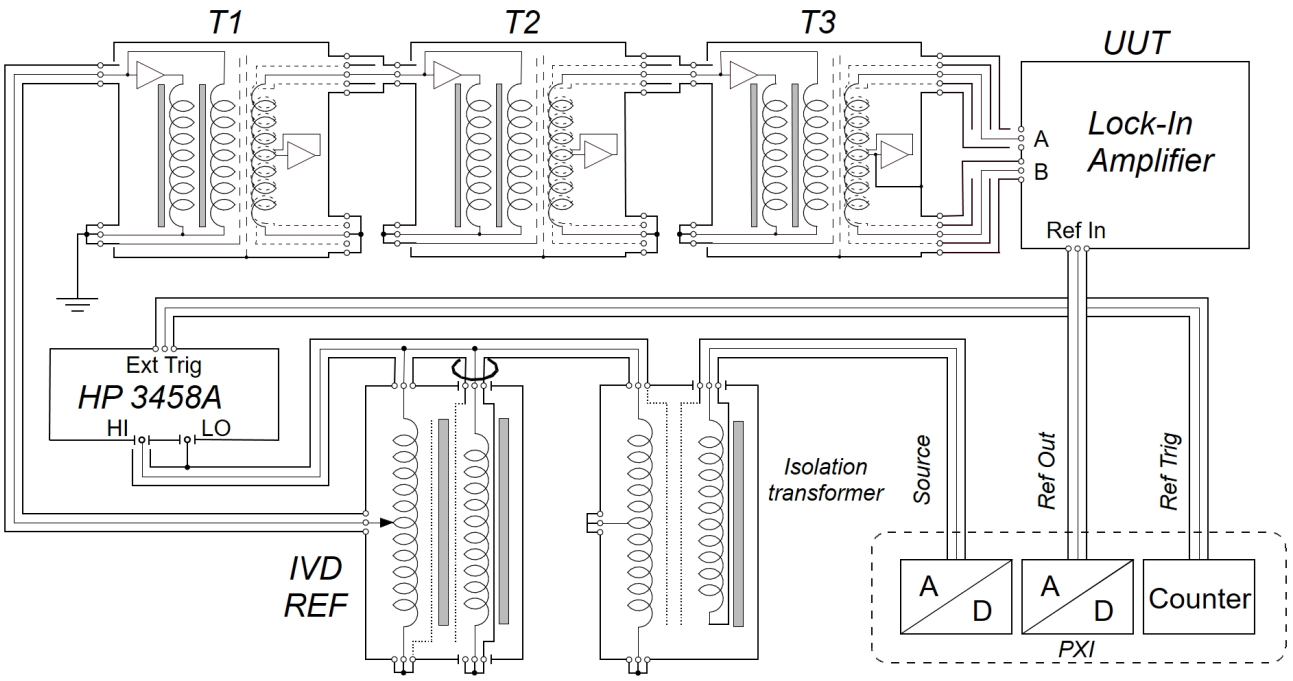

Figure 4. The METAS calibration setup. ©2019 IEEE. Reprinted, with permission, from [7].

determined according to (1): positive values of V_{CAL} correspond to $\varphi = 0$; negative values to $\varphi = \pi$. Due to time constraints, some of the measurements were limited to the positive values of V_{CAL}.

The error δ_{R}, which is relative to V_{CAL}, is approximately independent from V_{CAL}, whereas the error δ_{FS}, which is relative to V_{FS}, is approximately directly proportional to V_{CAL}. This suggests that the observed magnitude error is mainly due to a gain error of the lock-in amplifiers.

The uncertainty bars in the plots of δ_{R} and δ_{FS} corresponding to the INRIM setup are obtained by combining the type B component associated to V_{CAL} (discussed in section 4) and the type A components associated to the readings $V_{\mathrm{DUT}}^{\mathrm{read}}$ and $V_{\mathrm{OS}}^{\mathrm{read}}$ (the latter having a magnitude of 1 nV or less). The uncertainty of the METAS setup has been evaluated according with the previously published dedicated paper [7].

In the INRIM setup, the type B uncertainty associated to V_{CAL} is less than 100 pV (less than 1×10^{-4} relatively to V_{FS}), while the type A uncertainty associated to the DUT readings is at the nanovolt level (10^{-4}–10^{-3} relatively to V_{FS}). This means that the main contribution to the uncertainty of this calibration is given by the DUT itself. Similar results were obtained with the METAS setup.

The values of δ_{R} and δ_{FS} obtained from the INRIM and METAS calibration setups, which are quite different in terms of their implementation, are mostly compatible. A moderate mismatch in the calibration outcome of LIA1, for the specific case of $V_{\mathrm{FS}} = 10\,\mu\mathrm{V}$, can be observed in figures 5(c) (with a compatibility index less than 1.8) and 6(c) (with a maximum compatibility index of 3.8 at small magnitudes). This could be related to a possible instability of the specific DUT, since the same mismatch was not observed for LIA2 (figures 5(d) and 6(d)). Overall, both the DUTs were within the manufacturer specifications.

6. Conclusions

In this paper we presented a simple setup for the gain calibration of lock-in amplifiers which allows to reach a calibration uncertainty of the order of 10^{-4}, which is better by two orders of magnitude with respect to the typical manufacturer specifications.

The calibration signal is generated by a digital source and scaled down with cascaded inductive and resistive dividers. Commercial components are involved in the construction, and the measurement is automated. The source relative uncertainty is of parts in 10^5. The calibration uncertainty is limited by the noise and stability of the device under test. The best performances are achievable in the low frequency range (<1 kHz), but extensions to higher frequencies are possible by proper calibration of the dividers and loading effect corrections.

In the framework of the EURAMET Project 1466 *Calibration of lock-in amplifiers*, we arranged a bilateral comparison between the setup proposed

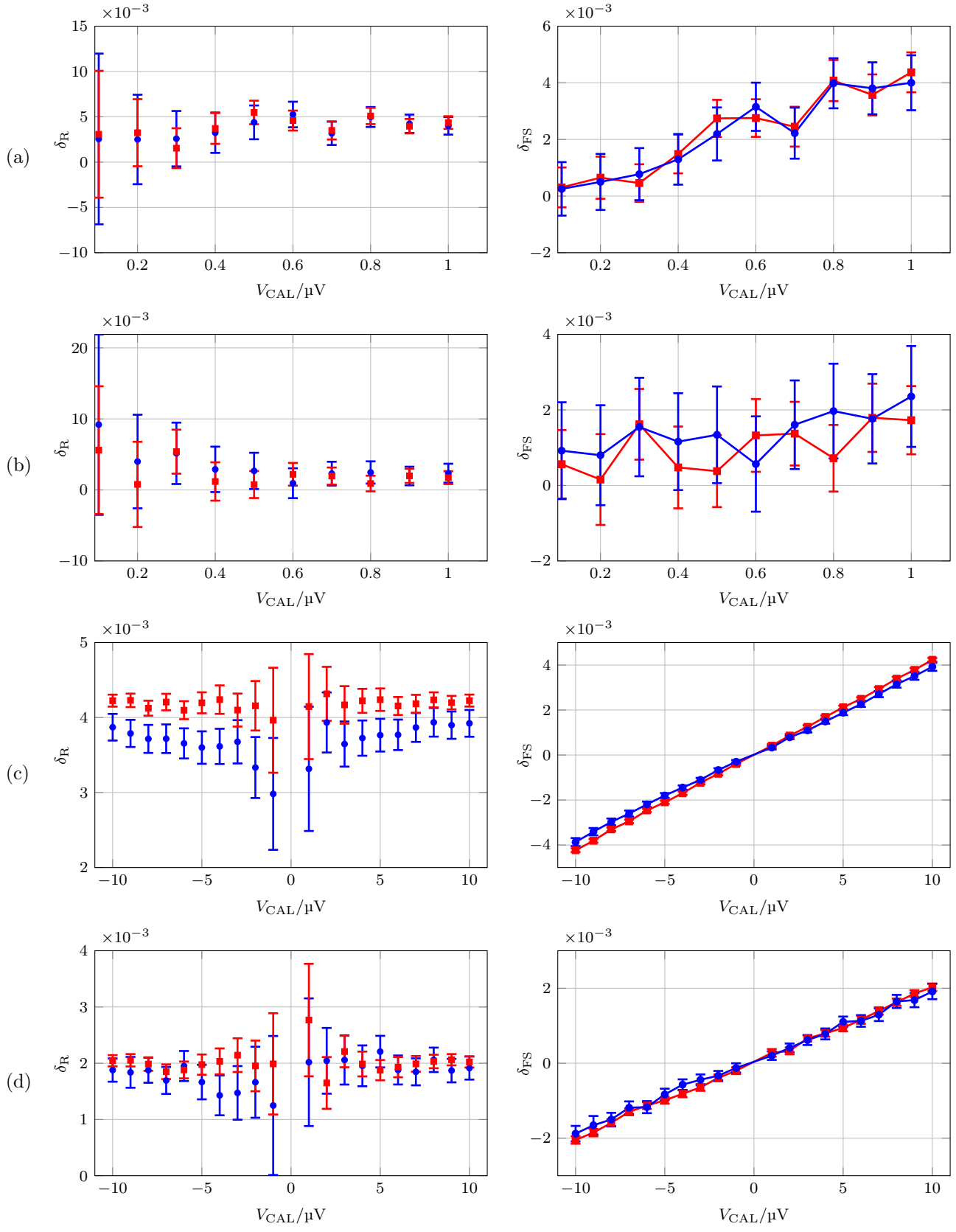

Figure 5. Results of the measurements performed at 20 Hz: (a) LIA1, 1 µV range; (b) LIA2, 1 µV range; (c) LIA1, 10 µV range; (d) LIA2, 10 µV range. In blue, with circle marks, the results obtained with the INRIM calibration setup. In red, with square marks, the results obtained with the METAS calibration setup.

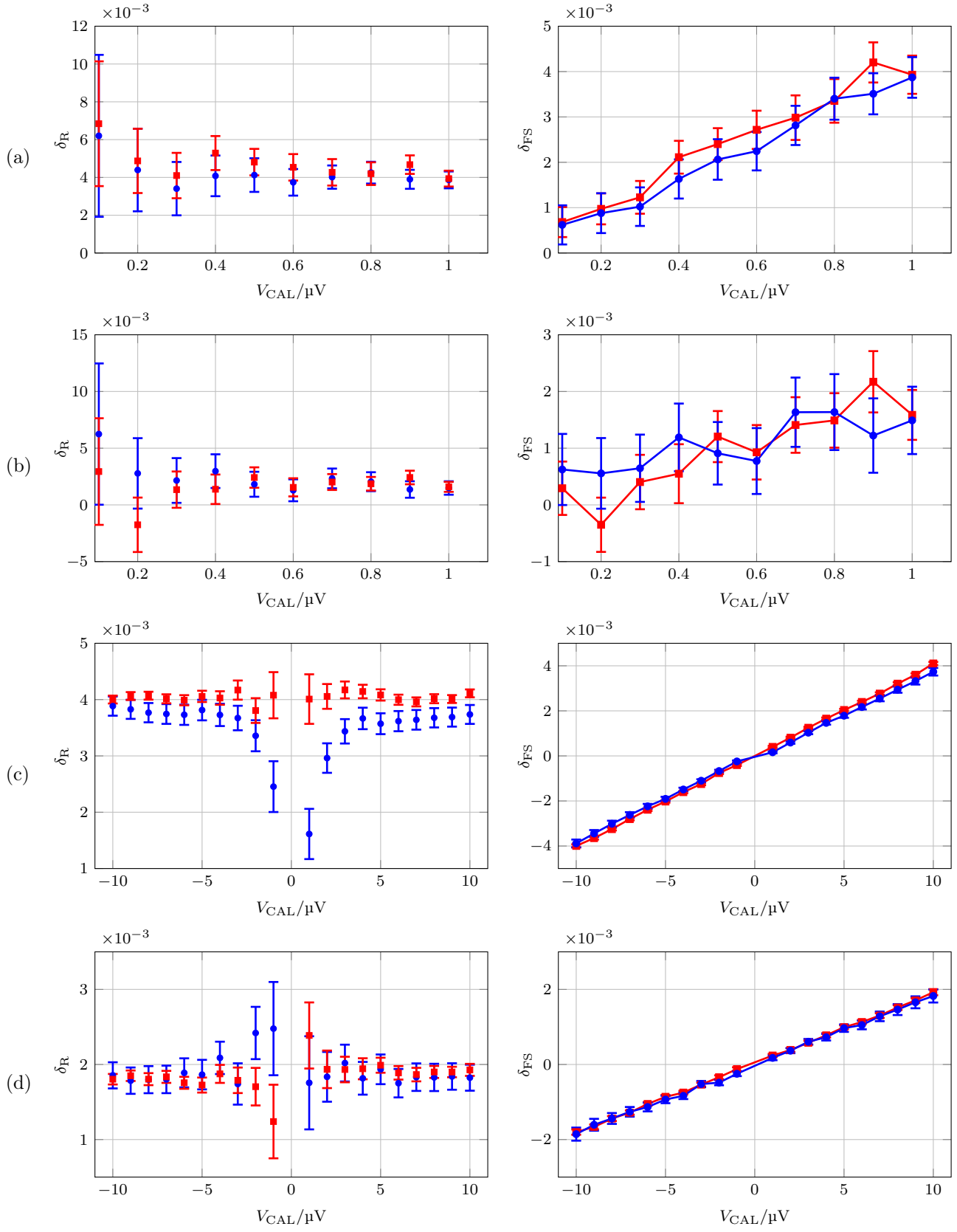

Figure 6. Results of the measurements performed at 103 Hz: (a) LIA1, 1 µV range; (b) LIA2, 1 µV range; (c) LIA1, 10 µV range; (d) LIA2, 10 µV range. In blue, with circle marks, the results obtained with the INRIM calibration setup. In red, with square marks, the results obtained with the METAS calibration setup.

and an existing one (section 5.1), based on a different design concept that involves purpose-built active transformers. The comparison, performed at METAS, consisted in the calibration of two digital lock-in amplifiers in the same laboratory environment. The outcome of the comparison, whose accuracy was limited by noise and stability of the instruments being calibrated, mutually validates the two calibration setups.

Acknowledgments

The authors thank Alessandro Mortara, METAS, for his support in the organization of the comparison, and Cristina Cassiago, INRIM, for providing LIA1.

References

[1] M. L. Meade, "Advances in lock-in amplifiers," *J. Phys, E: Sci. Instrum.*, vol. 15, no. 4, pp. 395–403, apr 1982.

[2] ——, *Lock-in amplifiers: principles and applications*, ser. IEE Electrical Measurement 1. London, UK: Peter Peregrinus Ltd., 1983.

[3] S. Tumanski, *Principles of electrical measurement*, ser. in Sensors. Boca Raton, FL, USA: Taylor & Francis, 2006, ch. 4.2.4, p. 154, ISBN: 978-0-7503-1038-3.

[4] L. Callegaro, *Electrical impedance: principles, measurement, and applications*, ser. in Sensors. Boca Raton, FL, USA: CRC press: Taylor & Francis, 2013, ch. 3.2.4.2, p. 67, ISBN: 978-1-43-984910-1.

[5] E. Theocharous, "Absolute linearity characterization of lock-in amplifiers," *Appl. Opt.*, vol. 47, no. 8, pp. 1090–1096, Mar 2008.

[6] F. Raso, A. Hortelano, and M. M. Izquierdo, "A calibration method of the linearity of lock in amplifiers," in *2016 Conf. Precis. Electromagn. Meas. (CPEM 2016)*, July 2016, pp. 1–2.

[7] D. Corminboeuf, "Calibration of the absolute linearity of lock-in amplifiers," *IEEE Trans. Instrum. Meas.*, vol. 68, no. 6, pp. 2060–2065, Jun 2019.

[8] D. Georgakopoulos, I. Budovsky, and S. P. Benz, "Josephson arbitrary waveform synthesizer as a reference standard for the calibration of lock-in amplifiers," in *2020 Conf. Precis. Electromagn. Meas. (CPEM 2020)*, Aug 2020, pp. 1–2.

[9] P. A. Probst and B. Collet, "Low-frequency digital lock-in amplifier," *Rev. Sci. Instrum.*, vol. 56, no. 3, pp. 466–470, 1985.

[10] F. Barone, E. Calloni, L. DiFiore, A. Grado, L. Milano, and G. Russo, "High performance modular digital lock-in amplifier," *Rev. Sci. Instrum.*, vol. 66, no. 6, pp. 3697–3702, 1995.

[11] H. Yao, K. Ema, and I. Hatta, "High-resolution AC calorimeter for measuring the heat capacity of small amounts of liquid samples," *Jpn. J. Appl. Phys*, vol. 38, no. 2R, p. 945, 1999.

[12] L. E. Bengtsson, "A microcontroller-based lock-in amplifier for sub-milliohm resistance measurements," *Rev. Sci. Instrum.*, vol. 83, no. 7, p. 075103, 2012.

[13] H. Yao, K. Ema, H. Fukada, K. Takahashi, and I. Hatta, "ac nanocalorimeter for measuring heat capacity of biological macromolecules in solution," *Rev. Sci. Instrum.*, vol. 74, pp. 4164–4168, 2003.

[14] G. de Graaf and R. F. Wolffenbuttel, "Lock-in amplifier techniques for low-frequency modulated sensor applications," in *2012 IEEE Int. Instrum. Meas. Technol. Conf.*, Graz, 2012, pp. 1745–1749.

[15] G. Macias-Bobadilla, J. Rodríguez-Reséndiz, G. Mota-Valtierra, G. Soto-Zarazúa, M. Méndez-Loyola, and M. Garduño Aparicio, "Dual-phase lock-in amplifier based on FPGA for low-frequencies experiments," *Sensors*, vol. 16, no. 3, p. 379, Mar 2016.

[16] T. J. Witt and N. E. Fletcher, "Standard deviation of the mean and other time series properties of voltages measured with a digital lock-in amplifier," *Metrologia*, vol. 47, no. 5, pp. 616–630, sep 2010.

[17] U. Pogliano, "Precision measurement of AC voltage below 20 Hz at IEN," *IEEE Trans. Instr. Meas.*, vol. 46, no. 2, pp. 369–372, April 1997.

[18] I. Robinson, J. Belliss, S. Bryant, A. Sánchez, Y. Álvarez, K. Schweiger, C. Díaz, M. Neira, L. Callegaro, R. D. Lee, I. Blanc, F. Overney, X. He, C. Ding, Z. Qian, B. Waltrip, G. Small, J. Fiander, P. Coogan, H. L. Johnson, Y. Nakamura, E. Dierikx, A. K. Saxena, M. Saleem, B. Wood, G. Ramm, G. Eklund, E. Turhan, and Y. Semenov, "Key comparison CCEM-k7: AC voltage ratio," *Metrologia*, vol. 49, no. 1A, pp. 01 007–01 007, jan 2012. [Online]. Available: https://doi.org/10.1088%2F0026-1394%2F49%2F1a%2F01007

[19] M. E. Briggs, R. W. Gammon, and J. N. Shaumeyer, "Measurement of the temperature coefficient of ratio transformers," *Rev. Sci. Instrum.*, vol. 64, pp. 756–759, 1993.

[20] G. Boella and G. M. Reedtz, "A room temperature setup to compare the quantized Hall resistance with 1-Ω standards," *IEEE Trans. Instrum. Meas.*, vol. 41, no. 1, pp. 59–63, 1992.

[21] N. Fletcher and R. Goebel, "The properties of commercial thick film resistance elements as ac-dc transfer standards," in *2008 Conf. Precis. Electromagn. Meas. (CPEM 2008)*, June 2008, pp. 110–111.

[22] *H series foil reistors datasheet, document number: 63006*, Vishay, Mar 2010. [Online]. Available: foilresistors.com

[23] *Model SR850 DSP lock-in amplifier*, 2nd ed., Stanford Research System, Jan 2009. [Online]. Available: thinksrs.com

[24] EURAMET project n. 1466, "Calibration of lock-in amplifiers," www.euramet.org.